Pre-coating of outside-inside capillary UF membranes with iron hydroxide particles to limit non-backwashable fouling during seawater algal blooms

Sergio G. Salinas-Rodriguez[a,*], Anjar Prabowo[a], Almotasembellah Abushaban[a], Ferdi Battes[a], Jan C. Schippers[a], Maria D. Kennedy[a,b]

[a]*Environmental Engineering and Water Technology Department, UNESCO-IHE Institute for Water Education, Westvest 7, 2611 AX Delft, The Netherlands, Tel. +31 152151780; email: s.salinas@unesco-ihe.org (S.G. Salinas-Rodriguez)*
[b]*Faculty of Civil Engineering, Delft University of Technology, Stevinweg 1, 2628 CN Delft, The Netherlands*

ABSTRACT

This research is structured on two hypotheses in which the first one is that pre-coating method using iron hydroxide particles in combination with ultrafiltration (UF) is able to control the non-backwashable (nBW) fouling in outside-inside UF membrane system caused by transparent exopolymer particles produced by marine algae species, *Chaetoceros affinis*. The initial assumption is that the success of the pre-coating method strongly depends on the uniform coverage of pre-coat material along the membrane surface that forms a protective layer. The second hypothesis is based on the presumption that a sequestering agent can avoid the growth of the iron hydroxide nanoparticles over time. Pre-coating experiments were performed with 6, 1, and 0.15 mg Fe^{3+}/L coagulant equivalent dose to synthetic seawater spiked with algal organic matter to assess its effect to membrane backwashability, especially the nBW fouling development. The results showed that all of the applied dosages for pre-coating were able to reduce the nBW fouling rate. Based on the observations, coating with 1 mg Fe^{3+}/L equivalent dose was the optimum dose to control the nBW fouling. It immediately stabilizes the fouling resistance from the first filtration cycle onwards. When a lower dose was applied, the stabilization occurred at lower rate. However, the success of pre-coating did not seem to be only attributed to a physical mechanism, (protective layer) but there is another mechanism that helps to control the nBW fouling. Results from SEM images supported this hypothesis by showing that the membrane surface was not fully covered by the iron hydroxide particles. It was an indication that there must be another mechanisms occurring in the pre-coating process.

Keywords: Pre-coating; Outside-inside; Ultrafiltration; Non-backwashable fouling; Iron hydroxide nanoparticles

1. Introduction

Inline coagulation and pre-coating are two known coagulant-based techniques that have been and still are popular subjects for researchers involved in the control of UF systems. Pre-coating and inline coagulation techniques can improve the membrane performance and also lower the coagulant use in UF systems [1–5]. Inline coagulation has better results in

*Corresponding author.

organic matter and turbidity removal efficiency than the pre-coating technique, thus it can provide a better permeate quality. Nevertheless, depending on coagulant dose used in the system, when it comes to fouling mitigation, previous research has shown that pre-coating UF membranes with a removable layer of particles at the start of each filtration run are more capable than inline coagulation for high salinity water [6]. Due to those facts, we propose in this work to test what pre-coating can offer to the UF membrane improvement.

Pre-coating is a method that is based on the formation of a thin layer on the surface of the capillary UF membranes; this layer can avoid direct interaction between the foulants and the membrane. Both physical and chemical interactions take place between coating material and the foulants such as transparent exopolymer particles (TEP) which have high adhesion properties. Recently, a study was presented demonstrating the utilization of iron hydroxide nanoparticles in inside-outside capillary UF systems during algal bloom event in seawater [3]. Aside from less coagulant used in the system, the study pointed out some other benefits of pre-coating with iron hydroxide nanoparticles, such as: (i) pre-coating can prevent direct fouling of the UF membranes with ferric hydroxide, thus less cleaning in place to remove iron, and (ii) it prevents direct fouling of RO with un-coagulated ferric hydroxide particles. Another point of consideration is the formation of the submicron particles for pre-coating. In the mentioned study, the submicron particles that were created by grinding the iron hydroxide flocs with high shear rates proved to have a better and more uniform membrane coverage, and were able to substantially lower the rate of non-backwashable (nBW) fouling development. Nevertheless, it was also reported that the nanoparticles were not stable in their size over time which could make the process not practical for on-site applications. In this study, we tested the effectiveness of pre-coating outside-inside capillary UF membranes with iron hydroxide nanoparticles outside-inside systems and we propose a method to control the size of the nanoparticles once they are formed to avoid their regrowth overtime. The market growth of ultrafiltration (UF) membranes has been forecasted to grow from $9 \, \text{Mm}^3/\text{d}$ permeate flow in 2014 up to $15 \, \text{Mm}^3/\text{d}$ in 2018 [7].

The interesting finding with regard to pre-coating is that only few researches can link the pre-coating with coagulation. Originally, this approach considered to pre-coat the membrane at the start of the filtration cycle, during a very short period of time and thereafter filtered the feed water through the coated membrane [1]. Other researchers did a similar experiment with more correlation to coagulation. Their experiments involved diluting a ferric chloride solution with ultra-pure water, dosed the slurry to the membrane until coating formed, and thereafter start the filtration cycle [4,8]. A recent approach demonstrated [3] involved the combination of Fe^{3+} precipitation and flocs grinding before dosing it to the membrane system. Pre-coating has been reported that can reduce the use of coagulant in UF membrane systems [3,4], particularly, when applying an iron hydroxide submicron particle layer in the range 0.2–1.5 µm with a low equivalent coagulant dose (0.5–1 mg Fe^{3+}/L) reduced significantly the nBW resistance in an inside–outside filtration system [4]. However, it was reported that the formed nanoparticles regrow over time [3], which is undesirable for an effective coating on the membrane surface and the coating process takes several minutes and also for the possibility of creating large volumes of nanoparticles at once, thus becoming a focus that will be addressed in this study. The other focus in this study is to investigate whether the coating phenomenon is able to reduce the nBW resistance in outside-inside UF system.

This work is structured in two hypotheses. The first one is that pre-coating using iron hydroxide particles in combination with UF is able to control the nBW fouling of outside-inside capillary UF membrane systems caused by algal organic matter (AOM) produced by marine algal species (*Chaetoceros affinis*, produced with North Seawater). The initial assumption is that the success of the pre-coating method strongly depends on the uniform coverage of pre-coat material along the membrane surface. The second hypothesis is based on the presumption that a sequestering agent (SA) can control the size of the iron hydroxide nanoparticles, which will help the production of nanoparticles in large volumes.

2. Methods

2.1. Formation of iron hydroxide nanoparticles

The procedure to prepare the iron hydroxide nanoparticles included standard procedure for floc formation: (i) rapid mixing with 208 rpm for 30 s and simultaneous pH correction with sodium hydroxide (1 or 6 M) until it reached a value of 10; (ii) slow mixing with 18 rpm for 15 min; (iii) grinding the solution at gradient velocity of around $12,000 \, \text{s}^{-1}$ for 2 min. The size measurements were performed with the Zetasizer NanoZS (Malvern, UK).

All the pre-coating and nanoparticle stabilization experiments used iron stock solution (3 g Fe^{3+}/L). The iron stock solutions were prepared by adding 14.52 g ferric chloride ($FeCl_3 \cdot 6H_2O$) into 1 L of demineralized water.

Pre-coating was performed with various coagulant equivalent doses (6 mg Fe^{3+}/L, 1 mg Fe^{3+}/L, and 0.15 mg Fe^{3+}/L) and tested on artificial seawater (ASW, as reported by other researchers [9,10]) spiked with AOM (concentration of 0.5 mg-C/L as biopolymers representative for algal blooms [11]). In this work, the equivalent doses are expressed as mg Fe^{3+}/L.

2.2. Filtration setup

For the study, a filtration setup (Fig. 1) was developed by following the membrane manufacturer's specifications. The increase in fouling resistance was monitored over time. The piston pumps (Pump 33, Harvard Apparatus) are able to deliver stable constant flow up to 4 bar of pressure. The pressure sensor (P) used was the model Cerabar M-PMC51 from Endress & Hauser.

The filtration experiment consisted of five processes, namely: (i) the procedure to determine clean membrane resistance, (ii) fouling propensity of AOM without pre-coating, (iii) fouling propensity of AOM with pre-coating, and (iv) fouling propensity of AOM with pre-coating and SA. The overall operating conditions and dose of coagulant and SA used in the filtration experiment can be seen in Table 1 below.

2.3. Feed water

Feed water used in the experiment contained AOM from seawater AOM, *Chaetoceros affinis*, which was cultured and cultivated in a pilot plant located in Jacobahaven, Zeeland. The pure AOM solutions were subjected to pre-filtration using 5 μm filter paper prior to being used for filtration experiment and characterization. Table 2 shows the main characteristic of the

Table 1
Operating conditions for filtration experiment

Parameter	Value
Filtration and pre-coating flux	100 L/m²/h
Number of cycles	6–7 cycles
Duration of one filtration cycle	30 min
Backwash flux	150 L/m²/h
Duration of backwash cycle	120 s
Coagulant equivalent dose	12, 6, 1, and 0.15 mg/L
Air flow rate	12 L/h
Sequestering agent dose	30 mg/L
Grinding intensity	12,000 s^{-1}

pure AOM solutions. Beside the liquid chromatography coupled with organic carbon detection (LC-OCD) technique, all parameters were measured at UNESCO-IHE's laboratory. The feed solutions were prepared by diluting the pre-filtered pure AOM solutions with ASW on the basis of total organic carbon (TOC) concentration.

LC-OCD measurements were conducted at DOC-Labor (Karlsruhe, Germany) to characterize the pure AOM solutions concerning the concentration of biopolymers and low molecular weight organic substances such as humics, acids, building blocks, and neutrals. This method does not consider the biopolymer concentration as a direct measure of TEP but more like a relative indicator of the amount of TEP and their colloidal precursors in the water sample [12]. The result for the LC-OCD is presented in Table 3.

The pure AOM solution comprised 2.42 mg-C/L of biopolymers, which is only 27.3% out of the total chromatographic DOC measured. The biopolymer fraction of this pure AOM is predominated by polysaccharides which explains there are only small fractions of organic carbon concentration of protein-like substances (0.75 mg C/L) in that solution. The high amount of low molecular weight compounds in the building block fraction might relate to the way the AOM was cultured in the Zeeland pilot plan, considering the nutrition that was fed to the algae species. That might explain the relatively high concentration of ethylenediaminetetraacetic acid (EDTA), which is commonly used as one of the substances for seawater algae media that appeared in the LC-OCD results.

Fig. 1. Schematic of the filtration setup for capillary UF outside-inside filtration.

2.4. Membranes

Commercial UF capillary polyvinylidene fluoride (PVDF) membranes with a nominal pore size of 0.03 μm and operating in outside-inside mode were used in this research. Prior to each experiment, a
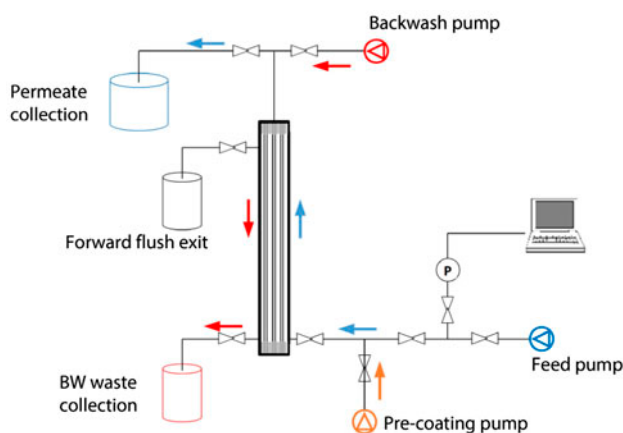
Table 2
Pure AOM solution characteristic

Parameters	Unit	Average value	Standard deviation
TOC	mg/L	10.5	0.1
Flow cytometry	cells/mL	2,340,000	–
Turbidity	NTU	0.75	0.021
pH		8.19	0.014
Temperature	℃	20	–
UV254	Abs/cm	0.194	0.001

Table 3
Pure AOM solution—LC-OCD analysis in mg/L

CDOC	Biopolymers	Humics	Building blocks	LMW neutrals	LMW acids
	(>>20,000 Da)	(<1,000 Da)	(300–500 Da)	(<350 Da)	(<350 Da)
8.87	2.42	0.45	3.51	1.48	0.99

membrane module (25 cm length, diameter 6 mm containing 6 fibers) was prepared manually in the laboratory.

The membrane resistance was measured with demineralized water and with artificial inorganic seawater (ASW). For both solutions, the normalized membrane resistance at 20℃ was the same with a value of 9.5×10^{11} per meter.

2.5. Particle size measurements

The Malvern Zetasizer Nano ZS was used to measure small particles (detection limit 0.0003–10 μm). The measurement is based on dynamic light scattering. In the measurement, several parameters influence the results, such as: viscosity, ionic strength, surface structure of the particles, angle of measurement, refractive index, absorbance of incident light, scattering intensity, and settling time of particles.

Due to turbidity and polydispersity of the samples, the measurements were conducted with two approaches: (i) measure the sample without filtering it, and (ii) filtering the samples with a 0.45 μm filter prior to measurement.

2.6. Stabilization of the regrowth of nanoparticles

The particle stabilization experiment starts with the formation of iron hydroxide nanoparticles. The coagulant dose used for this experiment was fixed at value of 10 mg/L, while for the SA the dose was fixed at 30 mg/L, as a proof of principle. The SA was added to the coating suspension immediately after 5 min grinding. Afterward, the mixed suspension was subjected to grinding for another 2 min to create a uniform solution. To monitor the regrowth of the nanoparticles after the grinding step, three measurements were taken over time (0, 50, and 90 min). Triplicate measurements were performed. The longer the formed particles remain stable in size (no regrow), the more of them can be produced at once.

2.7. Backwashable and nBW fouling rate

Backwashable (BW) fouling is the fraction of fouling that can be removed by a hydraulic backwash, while the nBW fouling is the fraction that cannot be removed only by a hydraulic backwash.

BW fouling rate is defined as the average slope of a linear regression of the last resistance values before backwash in successive filtration cycles as a function of time, while the nBW fouling rate is defined as the average slope of a linear regression of the initial resistance values after backwash as a function of time in successive filtration cycles.

3. Results and discussion

3.1. AOM fouling propensity

The fouling propensity of AOM solution was measured at two different concentrations (0.5 and 2 mg-C/L as biopolymers). AOM concentration of the feed solution plays an important role in fouling propensity. Although with relatively few cycles, the exponential development trend with the higher concentration (2 mg/L) was more pronounced compared to the lower concentration (0.5 mg/L) as can be seen in Fig. 2. A possible explanation that at higher AOM
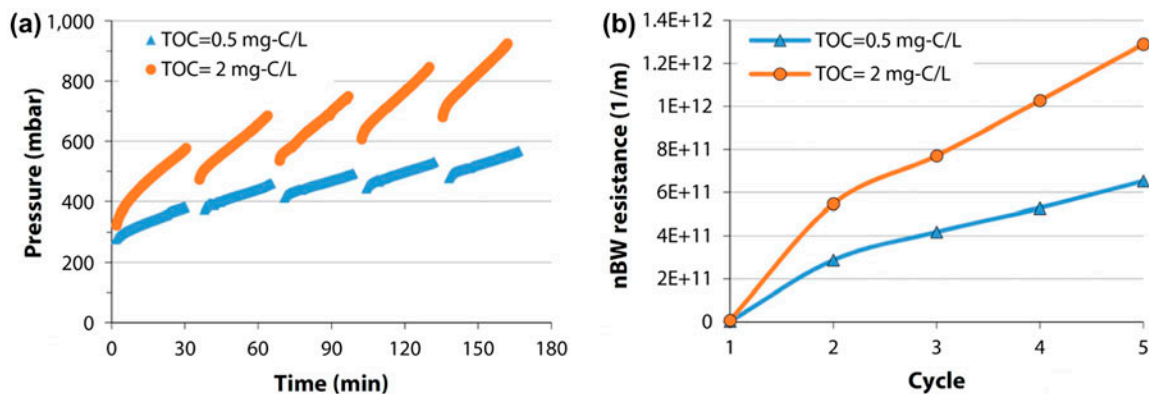
Fig. 2. Filtration of AOM solution (a) and nBW fouling rate (b) at different biopolymer concentrations.

concentration the pressure development deviates from linear trend is related to the dominant fouling mechanism which has been reported as cake compression or gel filtration [13,14], which resulted in a steep pressure development in such a short time. Furthermore, measurements performed at 0.5 mg-C/L showed a pressure increase in 0.29 bar within 5 cycles. Measurements performed at 2 mg-C/L showed an increase in the pressure at 0.59 bar within 5 cycles. Therefore, with four times higher feed concentration, the increase in pressure is twice as much.

Concerning the backwashability, Fig. 2(b) shows the nBW resistance increase within 5 cycles for the two biopolymer concentrations. The development of the nBW resistance has a strong correlation with the pressure development increase (Fig. 2(a)) for both feed water concentration. The observed increase in nBW over the filtration cycles suggests that the applied backwash was not effective in removing the foulants (sticky AOM) through successive cycles. The attachment of sticky AOM resulted in a reduction in effective filtration area due to complete pore blocking. To compensate for lower effective membrane area (due to fouling) while keeping constant the flux rate, the local velocity where filtration occurs need to increase creating thus higher local flux rates. The combined application of air scour and backwash should be tested as it could be more efficient in restoring permeability after each cycle.

The modified fouling index-UF (MFI-UF, [10,14,15]) at constant flux was calculated to illustrate the fouling potential of the feed water solution with 0.5 mg-C/L. The feed water fouling potential of that concentration need is calculated considering the 0.5 mg-C/L was the concentration being used for all the filtration experiment in this study. The calculated MFI value for that particular concentration is 8,790 s/L^2. This value is more than two times higher than the one reported

($3,500$ s/L^2) by other researchers who tested the same AOM for water with 0.5 mg/L biopolymer concentration [3]. The MFI-UF values could explain the phenomenon concerning the relatively high pressure development profile of the AOM used in this experiment compared with the ones obtained in the same reported work.

All the conducted experiments considered only the hydraulic backwashing with permeate water without the addition of air scour.

3.2. Effect of equivalent dose on UF operation

The pre-coating of the outside-inside membranes was applied in different equivalent doses which are presented in Table 4. The results show a positive effect of pre-coating for the outside-inside UF membrane, especially on the nBW rate development. The pre-coating experiment started with higher equivalent dose to prove the principle of coating mechanism. Afterward, the equivalent dose was lowered to find out which was more efficient to improve the nBW fouling rate, and at the same time to determine the lower limit of equivalent dose when the effect becomes similar with the higher dose.

The pre-coating experiment was conducted with 0.5 mg-C/L (TOC-based) biopolymer concentration on

Table 4
Applied equivalent dose

Coating suspensions concentration	Equivalent dose	Coating load
mg Fe^{3+}/L	mg Fe^{3+}/L	(mg/m^2)
4.5	0.15	7.5
30	1	50
180	6	300

feed water solution. Based on the experimental results presented in Fig. 3, AOM filtration without any pre-coating resulted in a steep increase in the pressure development profile within 7 cycles. In the same figure, it can be seen that the application of pre-coating in any equivalent dose reduced the pressure development significantly, especially for the nBW resistance through successive cycle. The effect of pre-coating immediately takes place from the first cycle onwards.

The pre-coating with 1 mg/L equivalent dose is the most notable dose to improve the nBW resistance. The resistance profile became similar to 6 mg/L equivalent dose when the 0.15 mg/L applied in the filtration. That is an indication that there is a certain limit when a low dose of coagulant dose is applied for coating. The interesting part is that in the first two cycles, the resistance increase is in the same range of value and started from the third cycle onwards. From there on, separation can be seen per different dosage concentrations. For the 6 mg/L equivalent dose, a consistent linear development was observed from the beginning, while for the 0.15 mg/L dose the resistance becomes stabilized and flattened at the fourth cycle onwards. Moreover, fast stabilization occurs at an equivalent dose of 1 mg/L from the first cycle onwards.

A hypothesis that can relate with the aforementioned result is that more uniform coverage occurs with the 1 mg/L, thus the effect of coating takes place immediately which is also in agreement with the results reported for inside-outside pre-coating [3]. For the higher equivalent dose, 6 mg/L, the formed sub-micron particles might be too large to be able to arrive at the membrane surface. On the other hand, with the lower equivalent dose (0.15 mg/L), the late stabilization might be due to the smaller particle not attaching properly on the membrane surface within a short period of time, but with time the filtration cycle forces

these small particles to the membrane surface to form a proper coating layer, thus the resistance started to stabilize. Additional experiments should be carried out to confirm the size of the particles generated by different doses.

An effect of pre-coating to the reduction of MFI-UF is presented in Fig. 4. The results show quite a significant reduction in MFI-UF, which is around four times lower for any equivalent dose than for filtration without pre-coating. The MFI-UF value for all equivalent doses is still in the same range, which is around 2,000 s/L^2. This finding is slightly different from the one reported by other researchers [3] which showed that the higher the equivalent dose, the lower the MFI-UF. This behavior was attributed to the occurrence of depth filtration in the coating, thus when the layer is thicker, the MFI-UF value decreases. However, that phenomenon is not likely to occur in outside-inside membranes, especially the membrane elements with relatively high packing density. With that condition, the formation of a coating layer is more
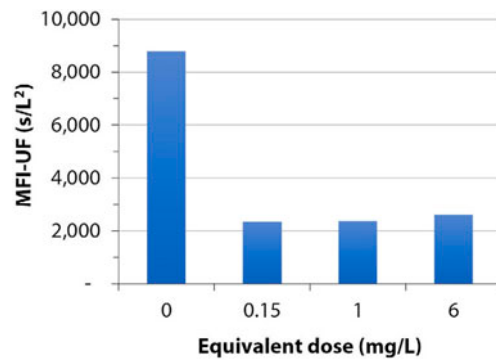

Fig. 4. Effect of pre-coating to MFI-UF 10 kDa measured at 120 L/m^2/h.
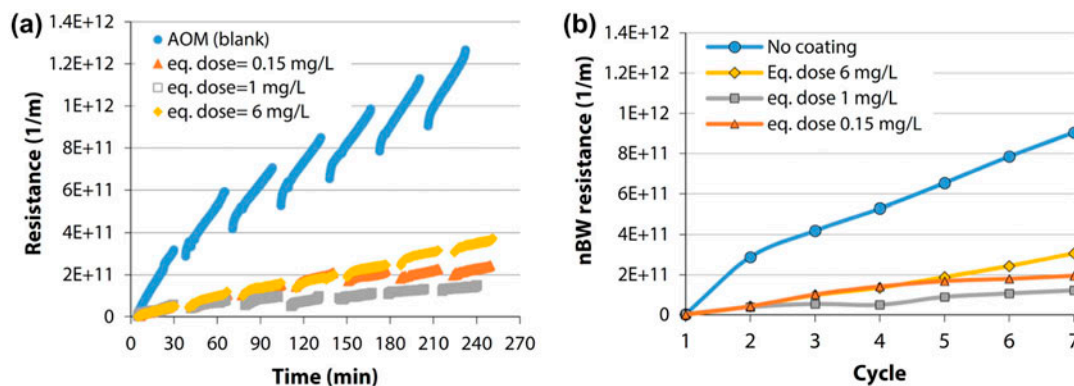

Fig. 3. Effect of coating equivalent dose on resistance (a) and nBW fouling build up resistance (b) in outside-inside UF.

challenging compared to inside-outside. In high packing density, it is unlikely that the coating will be formed on the side of fibers which are entwined to one another, thus there is no such condition that allows depth filtration by coating the layer in outside-inside.

The results show that pre-coating was effective in controlling the nBW fouling rate. The pre-coating with 1 mg/L equivalent dose produced the best results in terms of nBW fouling; this dose stabilized the fouling resistance from the first filtration cycle. When a lower dose was applied, the stabilization started at a lower rate.

3.3. Coating layer characterization

Membrane coating strongly depends on the uniform coverage of the pre-coat material along the entire membrane surface in a short period at the beginning of the filtration cycle. To verify the coverage of the pre-coat layer over the membrane, a visual observation using a scanning electron microscope (SEM) was conducted for the bottom and the upper part of the pre-coated membrane fibers used in this experiment. The membrane was pre-coated with an equivalent dose of 12 mg/L in the beginning of one filtration cycle only. Based on the longitudinal visual observation shown in Fig. 5, it seems that the membrane surface for both parts was not fully covered. That

condition might occur because the composition of formed larger particles was higher than the small particles. Previous researchers stated that the smaller particles will make a wide and even distribution on membrane surface while the larger particles will not deposit until they are at a certain distance from the capillary inlet [16]. Also, recently was reported [3] that particles formed with the highest shear rate (smaller particles) deposited relatively uniformly, while for the particles produced with lower shear rates (larger particles), the deposition was substantially less uniform.

The floc formation with equivalent dose of 12 mg/L was observed prior to grinding. Based on that observation, the flocs that formed prior to grinding were considered to be relatively big and concentrated flocs. The size of the formed flocs prior to grinding relates strongly to the size of submicron particles formed after the grinding process. A recent work reported similar uneven coating distribution in inside-outside membranes and also that with the same grinding intensity, the higher coagulant dose produced larger particles than the one with lower coagulant dose [3]. That could explain why the membrane surface shown in Fig. 5 was not fully covered by the coating particles.

Another reason that the membrane surface was not fully covered is because of the packing density of the fibers inside the membrane module. As mentioned previously, there are six fibers inside each 8 mm
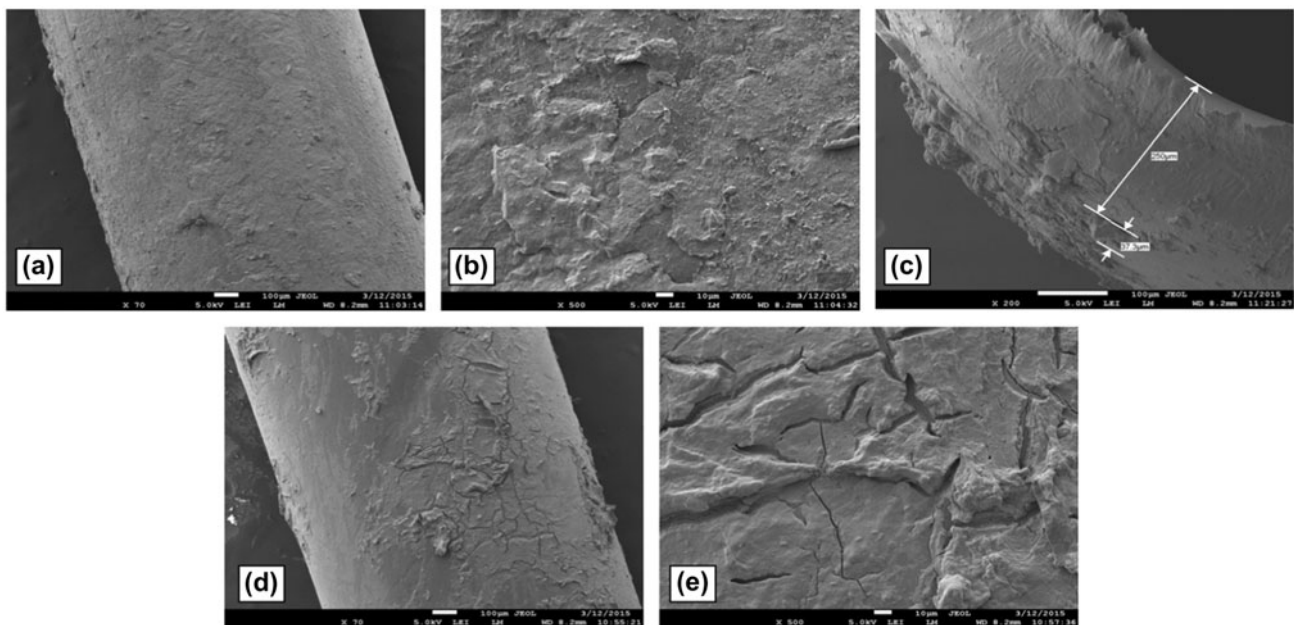

Fig. 5. SEM images of pre-coated capillary UF outside-inside membranes. (top of the fiber: (a) and (b)) (bottom of the fiber: (d) and (e)) ((c): cross section).

module, which is considered to be quite dense. Based on visual observation, the position of the fibers inside the module could be entwined with one another. This condition makes the deposition of pre-coat material on the membrane surface uneven along the length. On one side, the particles can deposit more while on the other side of the fibers, there is almost no particle deposition or at least much less. This particular situation needs to be taken into account when coating is applied in such a filtration system, especially in real applications, where 9,000 fibers per module are used, which makes a packing density much higher than the one used in this lab-scale study. This occurrence can also be caused by low surface porosity of the membrane fibers used in this experiment, which make it hard for the pre-coat material to coat the membrane surface uniformly.

Concerning the deposition of iron particles along the membrane, the bottom part of the outside-inside fibers seems to have more iron deposition compared to the upper part of the membrane. That result was already expected from the beginning. The membrane design used in this experiment allowed the iron particles to deposit more at the bottom part of the fibers than at the upper part of it. Ideally, the coating layer and the foulants attached on it will be flushed out during the backwash process. However, with the membrane design used in this experiment and the limitation of backwash process, it is believed that some coating particles remain on the membrane surface, especially at the bottom part of the membrane module.

Cross section SEM images of the pre-coated membrane fibers were also subject of observation. The cross section illustrates the thickness of the coating layer on top of the membrane surface. As can be seen in Fig. 5(c), the coating on the membrane surface is not evenly distributed. Nevertheless, the thickness of the coating layer (equivalent dose of 12 mg/L) on membrane surface is around 8–45 μm, which were considered to be relatively thick layers. As comparison, for a lower coagulant equivalent dose (3 mg/L) the thickness layer resulted in thinner layers (4.3 μm) [3]. Those differences, once more act as a proof that with less coagulant dose, the thinner the coating layer can be formed on membrane surface.

3.4. Particle stabilization

Measurement of the iron hydroxide particles after grinding was conducted to illustrate not only the particle regrowth over time, but also as a proof of principle that the SA can prevent the particle regrowth after the shearing/grinding process.

The measurements without the addition of SA were carried out with coagulant dose of 10 mg/L, where this value was based to compare our results with the other ones presented with inside-outside UF membranes [3]. The grinding step with coagulant equivalent dose of 10 mg/L with the same grinding intensity used in this study ($12,000 \text{ s}^{-1}$) resulted in a particle size with an average value of approximately 990 nm [3]. When the same coating suspensions measured again 10 min after grinding, it was determined that the particles size was above the detection limit of the zetasizer, which indicated that the particles grew in a relatively short period of time (Fig. 6).

The particle measurement for this experiment without filtering the coating suspension resulted in an average particle size of 1,953 nm immediately after grinding, which is bigger than reported [3]. Contrary to the same reported research, the particles that were being filtered prior to measurement resulted in a much smaller average particle size of 390 nm; this was expected because filtration prior to measurement partially removed the sedimenting particles which can interfere with the measurement. However, based on the measurement, the regrowth of particles over time is more pronounced if the samples are not filtered prior to analysis. In that case, the particles were growing to an average size of 7,529 nm at 50 min after grinding, and even much bigger at 90 min after grinding, which is 79,450 nm in average size (Fig. 6). On the other hand, the regrowth of particles when being filtered was less pronounced, which may be caused by the side effect of the filtration itself that made the particle dispersity in the suspension too high. That condition also can interfere with the measurement. Nevertheless, in either case, especially the unfiltered
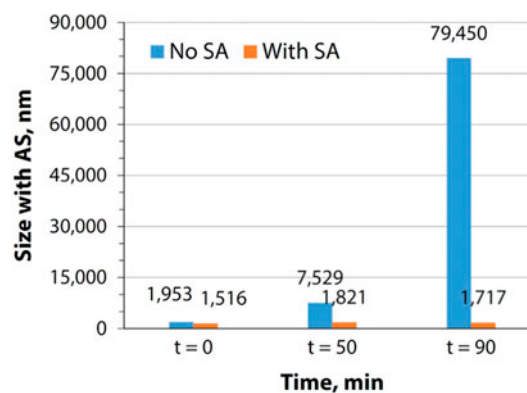

Fig. 6. Average size of particles over time (pH 10, coagulant dose: 10 mg Fe/L, rapid mixing: 30 s, slow mixing: 15 min, grinding time: 5 min, SA dose: 30 mg/L, backward scattering).

suspension verified that the iron hydroxide particles indeed get bigger over time after the grinding process.

The average size at time zero (initially after grinding) was around 1,953 nm. It was observed that the particles grew over time, as illustrated in Fig. 6. 30 mg/L of SA dose was able to keep the iron hydroxide particles within the same range of size over time.

To support the measurement results by Zetasizer, a simpler indicator, namely turbidity was measured over time after the grinding process. The result for both approaches, unfiltered and filtered, shows an increase in the turbidity value over time, which is an indication that the number of particles in the suspension increased. The summary of the measurements can be seen in Tables 5 and 6.

An increase in turbidity means an increase in scattered light. The larger a particle, the more light can be properly scattered back. This is most likely an increase in size and not in particle count. It is possible that the total amount went down due to aggregation.

The increase in count rate (total amount of photons on detector per time index) between $t = 0$ and $t = 50$ shows that particles are growing a bit. The decrease at $t = 90$ shows that part of the particles are no longer scattering back. This could mean that there is a settling of particles. That theory makes sense when regarding the starting value of the correlation coefficient. The higher this value is (at least higher than 100%), the more settling/sedimentation has occurred during the measurement. These results suggest that particles have grown (based on total count rate), and part of them have settled (based on total count rate and the starting value of the correlation coefficient).

An increase in the count rate shows that the particles are growing (yet very slowly). All of the measurements were performed with the maximum of light possible for the reflection. Even then, for all measurements not more than 100 photons were detected per second (this is very low). All starting values of correlation coefficients are less than 100% (meaning that there might be large deviations in the results due to interferences, however small these might be). The ratio between measured peak mean and polydispersity index (PdI) shows that all results can be considered to be more or less the same. Using the results is not to be advised, since PdI's are larger than measured values, and total counts are too low to accurately use a value. We can see that the total count rate goes up in time. This could be due to particle regrowth in time.

Both filtered and unfiltered samples showed forms of regrowth in time. Due to the fact that most of the produced particles at time 0 are larger than 0.45 µm (cut off size of the filters used), the results of the filtered samples cannot be used. These did not contain enough particles for proper measurement.

After it was indicated that indeed the iron hydroxide nanoparticles regrow over time, the SA experiment was conducted. As explained previously in this work, the hypothesis is that the SA can control the regrowth of the grinded particles, forming a complex bond and keeping the iron hydroxide nanoparticles in solution, instead of in precipitation presence. In other words, to illustrate whether the SA can stabilize the iron hydroxide nanoparticles in submicron size after the grinding process. A very high dose of SA, 30 mg/L, was added as a proof of principle. The measurement result supported the initial hypothesis. Based on measurements, for both unfiltered and filtered, it seems that at 50 and 90 min after grinding, the particles stabilize and remain in the same size range compared to the one

Table 5
Unfiltered iron hydroxide nanoparticles measurement

Type	PdI	Pk 1 mean (nm)	Total counts	Starting correlation coefficient (%)	Turbidity (NTU)
Without SA ($t = 0$)	1	1,035	3,126	100	9.13
Without SA ($t = 50$)	1	1,276	3,257	180	9.97
Without SA ($t = 90$)	1	1,273	2,775	340	10.4

Note: PdI = poly dispersity index; Pk = peak.

Table 6
Filtered iron hydroxide nanoparticles measurement

Type	PdI width	Pk 1 mean (nm)	Total counts	Starting correlation coefficient (%)	Turbidity (NTU)
Without SA ($t = 0$)	942	206	51	58	0.233
Without SA ($t = 50$)	1,643	172	58	78	0.322
Without SA ($t = 90$)	800	405	68	48	0.38

Table 7
Unfiltered iron hydroxide nanoparticles measurement with SA

Type	PdI	Pk 1 mean (nm)	Pk 2 mean (nm)	Total counts
With SA ($t = 0$)	564	1,175	5,108	3,905
With SA ($t = 30$)	802	1,515	5,366	4,157
With SA ($t = 60$)	676	1,265	–	4,139
With SA ($t = 120$)	555	1,190	–	4,019

Table 8
Filtered iron hydroxide nanoparticles measurement with SA

Type	PdI	Pk 1 mean (nm)	Total counts
With SA ($t = 0$)	257	271	77
With SA ($t = 30$)	160	289	102
With SA ($t = 60$)	211	318	108
With SA ($t = 120$)	278	338	103

which measured immediately after grinding. The indication was more pronounced with the unfiltered suspension than in the filtered one. That might suggest that the SA can react better with the iron hydroxide particles when there is more particulate iron in the suspension. The summary of measurements can be seen in Tables 7 and 8.

The first two measurements ($t = 0$ and $t = 30$) show there are two peaks, though the second peak disappears in time. This could be dust in the measurement cell that has been removed during the rinsing of this cell when applying the $t = 60$ sample. The average size deviation of peaks between 1,175 and 1,515 is smaller than the Polydispersity Indices from any of the measurements. The fact that the total amount of counts does not change significantly shows that the particles themselves do not grow in time.

All of the measurements were performed using the maximum amount of light possible (indicating that the total amount of particles that can scatter light is too low). It can be observed that the average measured size increases slightly in time, though polydispersity for all the measured time indices is higher than the total difference between $t = 0$ and $t = 120$.

For both filtered and unfiltered samples, an actual growth in time cannot be seen when SA is added. The samples appear to be quite stable.

4. Conclusion

Application of coating with different equivalent doses (6, 1, and 0.15 mg/L) in outside-inside UF system shows remarkable results concerning the improvement in nBW resistance through successive cycles.

Equivalent dose of 1 mg/L proves to be the optimum dose to control the nBW rate. It can immediately stabilize the resistance from the first filtration cycle. When a lower dose is applied, the stabilization occurs at slower rate.

Based on visual observations using SEM imaging, the membrane fibers were not fully covered by iron hydroxide particles. This is an indication that the success of reducing the nBW fouling cannot completely be attributed to physical mechanisms (coating layer), but also to a chemical mechanism.

The particle stabilization experiment showed that the submicron particles with size of 1,950 nm were formed immediately after grinding and they grew bigger over time. Moreover, the use of SA immediately after grinding gives a positive indication that it is able to stabilize the iron particles over time.

Smaller particles were formed when samples were filtered prior to measurement, but the effects of SA to stabilize the particles are more pronounced when samples were not being filtered.

The use of SA in filtration experiments worsen the nBW resistance profile when applied in 1 mg/L equivalent dose. Nevertheless, it gives an indication that it worked when applied at lower dose (0.15 mg/L).

References

[1] G. Galjaard, P. Buijs, E. Beerendonk, F. Schoonenberg, J.C. Schippers, Pre-coating (EPCE®) UF membranes for direct treatment of surface water, Desalination 139 (2001) 305–316.
[2] C. Guigui, J.C. Rouch, L. Durand-Bourlier, V. Bonnelye, P. Aptel, Impact of coagulation conditions on the in-line coagulation/UF process for drinking water production, Desalination 147 (2002) 95–100.
[3] S.A.A. Tabatabai, J.C. Schippers, M.D. Kennedy, Effect of coagulation on fouling potential and removal of algal organic matter in ultrafiltration pretreatment to seawater reverse osmosis, Water Res. 59 (2014) 283–23294.

[4] P.-K. Park, C.-H. Lee, S.-J. Choi, K.-H. Choo, S.-H. Kim, C.-H. Yoon, Effect of the removal of DOMs on the performance of a coagulation-UF membrane system for drinking water production, Desalination 145 (2002) 237–245.

[5] K.Y.-j. Choi, B.A. Dempsey, In-line coagulation with low-pressure membrane filtration, Water Res. 38(19) (2004) 4271–4281.

[6] S.A.A. Tabatabai, Coagulation and Ultrafiltration in Seawater Reverse Osmosis Pretreatment, CRC Press/Balkema, Leiden, 2014.

[7] Global Water Intelligence, Market Profile: The Low-pressure Membrane Market, in Global Water Intelligence, Media Analytics Ltd., Oxford, 2014, pp. 45–47.

[8] M.M. Sharp, I.C. Escobar, Effects of dynamic or secondary-layer coagulation on ultrafiltration, Desalination 188(1–3) (2006) 239–249.

[9] T. Waly, M.D. Kennedy, G.-J. Witkamp, G. Amy, J.C. Schippers, The role of inorganic ions in the calcium carbonate scaling of seawater reverse osmosis systems, Desalination 284 (2012) 279–287.

[10] S.G. Salinas Rodríguez, G.L. Amy, J.C. Schippers, M.D. Kennedy, The modified fouling index ultrafiltration constant flux for assessing particulate/colloidal fouling of RO systems, Desalination 365 (2015) 79–91.

[11] L.O. Villacorte, S.A.A. Tabatabai, D.M. Anderson, G.L. Amy, J.C. Schippers, M.D. Kennedy, Seawater reverse osmosis desalination and (harmful) algal blooms, Desalination 360 (2015) 61–80.

[12] L.O. Villacorte, Algal Blooms and Membrane Based Desalination Technology, UNESCO-IHE/Delft University of Technology, CRC Press/Balkema, Leiden, 2014.

[13] S.F.E. Boerlage, M.D. Kennedy, M.R. Dickson, D.E.Y. El-Hodali, J.C. Schippers, The modified fouling index using ultrafiltration membranes (MFI-UF): Characterisation, filtration mechanisms and proposed reference membrane, J. Membr. Sci. 197 (2002) 1–21.

[14] S.G. Salinas Rodríguez, M.D. Kennedy, G.L. Amy, J.C. Schippers, Flux dependency of particulate/colloidal fouling in seawater reverse osmosis systems, Desalin. Water Treat. 42 (2012) 155–162.

[15] S.G. Salinas Rodríguez, B. Al-Rabaani, M.D. Kennedy, J.C. Schippers, G.L. Amy, MFI–UF constant pressure at high ionic strength conditions, Desalin. Water Treat. 10 (2009) 64–72.

[16] S. Panglisch, Formation and prevention of hardly removable particle layers in inside-out capillary membranes operating in dead-end mode, Water Sci. Technol. Water Supply 3(5–6) (2003) 117–124.